

PHYSICAL REVIEW C

NUCLEAR PHYSICS

THIRD SERIES, VOLUME 37, NUMBER 1

JANUARY 1988

${}^1\text{H}(\vec{d}, \gamma){}^3\text{He}$ reaction at $E_d = 95$ MeV

W. K. Pitts,* H. O. Meyer, L. C. Bland, J. D. Brown,[†] R. C. Byrd,[‡] M. Hugi,[§]
H. J. Karwowski,* P. Schwandt, A. Sinha,^{††} J. Sowinski, and I. J. van Heerden^{†‡}
Indiana University Cyclotron Facility, Bloomington, Indiana 47405

A. Arriaga and F. D. Santos

Centro de Fisica Nuclear da Universidade de Lisboa, 1699 Lisboa, Portugal

(Received 19 January 1987)

The tensor analyzing power A_{yy} , vector analyzing power A_y , and cross section $\sigma(\theta)$ of the reaction ${}^1\text{H}(\vec{d}, \gamma){}^3\text{He}$ have been measured at a deuteron energy of 95 MeV, corresponding to photo-disintegration with 37 MeV photons. The total cross section is in good agreement with ${}^3\text{He}(\gamma, p){}^2\text{H}$ measurements; A_y and A_{yy} were both small and negative. A_{yy} is known to be sensitive to the ${}^3\text{He}$ D -state amplitude, and all previous measurements of tensor analyzing powers have been made in an energy region where the initial state interaction between the proton and deuteron is strong. These data were interpreted using a plane-wave Born approximation model which has been successful in describing other measurements of A_{yy} at lower energies. Within the framework of this model, these measurements were found to be consistent with an asymptotic D - S state normalization ratio $\eta = -0.029$.

I. INTRODUCTION

The effects of small components of the nuclear wave function are usually emphasized in the polarization observables of a reaction, since the polarization observables are given by the interference of amplitudes. An example of this selectivity to certain small amplitudes can be found in the recent experimental and theoretical studies of the tensor analyzing powers of the reaction ${}^1\text{H}(\vec{d}, \gamma){}^3\text{He}$, which have been found to be strongly dependent on the small ${}^3\text{He}$ D -state component.¹⁻³ All previous measurements of the tensor analyzing powers in this reaction have been carried out at deuteron energies between 19.8 and 45.3 MeV, in an energy regime where the effects of initial state interactions between the deuteron and proton are strongest.^{4,5} At $E_d = 95$ MeV these initial state interactions should be much less important than at lower energies, since calculations of $\sigma(90^\circ)$ using the distorted-wave Born approximation (DWBA) tend to agree with these exact calculations for $E_\gamma \geq 30$ MeV. Obviously one would want to compare these new measurements of the tensor analyzing powers to Faddeev model calculations using realistic potentials. There has been a Faddeev model calculation of A_{yy} using the Reid soft core potential, but only at $E_d = 29.2$ MeV.¹ In this calculation it was found that practically all (95%) of the tensor analyzing power A_{yy} was given by the ${}^3\text{He}$ D -

state amplitude, with only 5% being due to the deuteron D state. When the Malfliet-Tjon III potential (which has no tensor force, and therefore will not mix the S -state and D -state components of ${}^3\text{He}$) was used in the calculation, A_{yy} nearly vanished. In the absence of such complete calculations at different energies, calculations which have used a Faddeev model ${}^3\text{He}$ wave function projected into the proton and deuteron channel have been used to interpret the experimental data.^{2,3} While all available calculations differ in approach, the sensitivity of the tensor analyzing powers to the D -state component of ${}^3\text{He}$ seems to be firmly established.

II. THE EXPERIMENT

This measurement was carried out at the Indiana University Cyclotron Facility. The experimental apparatus (Fig. 1) was placed symmetrically on opposite sides of the beam axis. Photons were distinguished by the time correlation between the photon detector signal and the cyclotron rf signal; detection of the coincident helium was required to distinguish radiative capture events from events due to carbon in the CH_2 target.

The major experimental problem to be solved was the design and construction of a suitable detector for these ${}^3\text{He}$ nuclei. Since the ${}^3\text{He}$ nuclei from the ${}^1\text{H}(\vec{d}, \gamma){}^3\text{He}$ reaction emerged at less than 3.7° away from the beam axis, the recoil detector was in an angular region with a

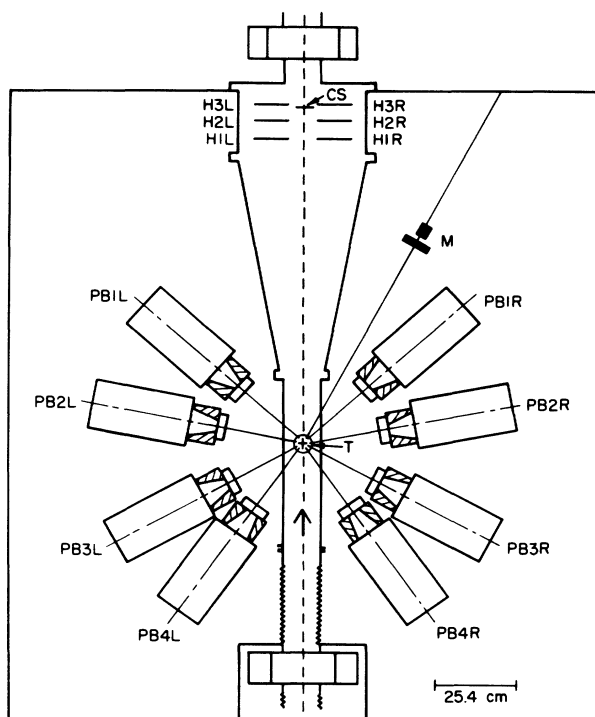


FIG. 1. Apparatus for study of the ${}^1\text{H}(\vec{d}, \gamma){}^3\text{He}$ reaction. Telescope elements, H1L through H3R. Lead glass Čerenkov detectors, PB1L through PB4R. Target, T; target monitor, M; alignment scintillator, CS.

large flux of deuterons scattered from the carbon in the target. Plastic scintillator telescopes were chosen since organic scintillators have very fast decay times, and thus are less sensitive to pileup. Each telescope consisted of three plastic scintillator paddles (Fig. 1, H1L through H3R). The first plane, H1L and H1R, was thin (0.068 cm), giving good pulse height discrimination between charge $Z=1$ and charge $Z=2$ particles; elastically scattered deuterons were eliminated by the threshold setting in this plane. The second and third planes were thicker (0.194 and 0.159 cm, respectively) and stopped all the ${}^3\text{He}$ nuclei from the ${}^1\text{H}(\vec{d}, \gamma){}^3\text{He}$ reaction. A candidate ${}^3\text{He}$ nucleus was required to give a coincidence between the first and second planes of the telescope. The size of the paddles was optimized with a Monte Carlo simulation of the detector response. This simulation predicted the detector response, and included effects due to multiple scattering and energy loss in the target. The code also accounted for the variation of the light output for different particle species.

Lead glass Čerenkov counters were used to detect the photons (Fig. 1, PB1L through PB4R). These detectors had a very good timing response of about 800 ps (full width at half maximum), of which no more than about 200 ps is due to the width of the beam pulse. Another advantageous feature of Čerenkov detectors is that neutrons can only be detected through a process such as $(n, n'\gamma)$. This combination of good timing performance and relative insensitivity to neutrons was ideal. Unfor-

tunately the pulse height resolution of these detectors is poor at these energies due to the small number of photons from the Čerenkov process. The typical pulse height resolution for a 32 MeV photon was only about 40%. The acceptance of these detectors (and the reaction angle) was defined by 7.6 cm thick lead collimators. The flux of charged particles was attenuated by 2.5 cm thick plastic absorbers located in front of the collimators.

Most of the random coincidences between the recoil telescope and the photon detectors were due to either deuteron reactions in the recoil telescope, evaporation particles of charge $Z=1$ from carbon, or multiple deuterons (in the telescope) from the same beam burst. Since the coincidence width between the photon detector and the recoil telescope was set to be three rf periods wide, a sample of random coincidences was acquired for later subtraction in the data analysis. Most neutron induced events in the photon detectors were eliminated by requiring that the photon timing signal and the cyclotron rf timing signal overlap to within 10 ns. The trigger conditions were that the photon signal have this 10 ns overlap and the recoil telescope signal have a larger pulse height than an elastically scattered deuteron. Events satisfying the trigger conditions were stored on magnetic tape. The dead time of the electronic system was measured by simulating events using light emitting diodes mounted on all detectors.

During off-line event reconstruction photons were identified by the correlation between a sharp time of flight relative to the rf system (1 ns or less) and a pulse height of (usually) 20 MeV or greater. Particles with charge $Z=2$ were identified on the basis of the correlation between the first plane pulse height and the pulse height sum in the recoil telescope. Radiative capture events in coincidence with an elastically scattered deuteron (in the same rf period) were characterized by a shift in the summed pulse height. A wide limit was set on the summed pulse height so that these events would be accepted. Since the timing signal from the first plane of the recoil telescope was unaffected by the deuteron, these events could still be identified as acceptable radiative capture events. All of the above conditions were applied to the time of flight spectra of the recoiling ${}^3\text{He}$ nuclei (Fig. 2), and these radiative capture peaks were summed.

The deuteron beam was of mixed vector and tensor polarization, and typical values of the vector and tensor polarization were $p_y=0.28$ and $p_{yy}=0.82$. The tensor polarization was cycled in 60 s intervals through each of the polarization states "unpolarized," "tensor positive," and "tensor negative." The vector polarization was reversed several times during the experiment. The polarization of the beam was measured immediately after the injector cyclotron where the beam energy is $E_d=8.8$ MeV and the ${}^3\text{He}(\vec{d}, p){}^4\text{He}$ reaction is an excellent analyzer. The polarization was not measured at the target, since there are no suitable analyzing reactions at $E_d \approx 95$ MeV.⁶ While it is possible for the spin alignment axis of the beam to shift from the vertical by a small amount during acceleration in the cyclotron, tests have shown that this shift of the alignment axis is less

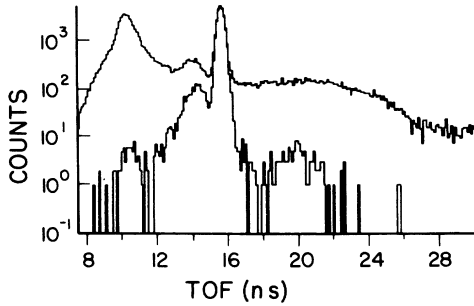


FIG. 2. Typical time of flight spectra for the recoil telescope, gated with and without the radiative capture conditions. The origin is the arrival time of a burst at the target. The large peak at 15.5 ns is due to the ${}^1\text{H}(\vec{d},\gamma){}^3\text{He}$ reaction, while the 14.0 ns ${}^3\text{He}$ nuclei are from the ${}^{12}\text{C}(\vec{d},{}^3\text{He})X$ reaction in random coincidence with a photon.

than 1° . The polarization at the target is then the same as that measured in the low energy polarimeter, to the extent that the beam is not depolarized during acceleration. Since sequential measurements of the beam polarization typically varied by less than the statistical uncertainty of the measurement, any systematic variation of the polarization measurements is estimated to be less than the statistical uncertainty. The statistical uncertainty in the polarization is taken to be that given by the statistical accuracy of a typical polarization measurement, which was usually about 3% for both the tensor and vector components. The uncertainty of the polarimeter calibration is estimated to give an error of less than 5% in the determination of the polarization.

Many false asymmetries in the analyzing power are cancelled by forming the ratio of the polarized yield to that from the unpolarized beam (normalized to the integrated beam current); for example, uncertainties in the detector efficiency or solid angle cancel. The vector analyzing power A_y was calculated from the left-right asymmetry for each of the two polarized states, while the tensor analyzing power A_{yy} was calculated for each side from the beam polarization-induced asymmetry. Averaging the analyzing powers (for the two states in the case of the vector analyzing power, and for the two sides in the case of the tensor analyzing power) then reduced the errors in the analyzing powers due to angular misalignment or errors in the determination of the polarization.

The yield ratios are still sensitive to the deadtime of the system, which could possibly vary as a function of beam polarization. The average dead time was only about 6% for all spin states. Another effect measured with the light-emitting diode (LED) pulser was the loss of counts in the ${}^3\text{He}$ peak due to random stops in the time to digital converter (TDC). A given event will have its timing peak shifted to an earlier time if the TDC is stopped by an earlier (uncorrelated) pulse. About 1% of the counts are shifted to earlier times, in good agreement with the expected shift based upon the singles rate in the first plane and the cyclotron rf frequency of 28.57 MHz. The background contribution from the carbon in the

CH_2 target was measured with a pure carbon target. Within the statistical precision of the background measurement, the carbon background under the peak had no polarization dependence.

Many effects were considered in the evaluation of the errors associated with the cross section measurement. Fortunately the ${}^1\text{H}(\vec{d},\gamma){}^3\text{He}$ reaction is much larger than the background, and it was possible, using tight sorting conditions, to make nearly pure samples of “tagged” ${}^3\text{He}$ nuclei or photons. Reaction losses in the telescope were determined from the low energy tail of the ${}^3\text{He}$ peak in the total pulse height spectrum, where it was found that about $1.5\pm 0.5\%$ of the ${}^3\text{He}$ nuclei did not deposit their full energy. This fraction of the ${}^3\text{He}$ sample is about the same as that predicted for nuclear reactions in the recoil telescope using the total reaction cross section.⁷ A similar procedure was used to estimate losses due to sorting cuts on the photon timing signal. Tight conditions from the recoil telescope response were used to gate the photon timing spectra and an estimated $99.5\pm 0.5\%$ of the ${}^1\text{H}(\vec{d},\gamma){}^3\text{He}$ events were inside the photon time window. The efficiency of the Čerenkov detectors for photon energies of about 20 MeV has been measured with tagged photons at the University of Illinois microtron and was found to be unity within experimental errors; a conservative efficiency of $98\pm 2\%$ is assumed for 30 MeV photons.⁸ Later tests at Illinois showed that the plastic absorbers lowered the efficiency to $96\pm 2\%$ for a software threshold of 20 MeV. The loss of events due to multiple scattering of the ${}^3\text{He}$ nuclei out of the telescope acceptance (due to carbon in the CH_2 target) was estimated with the Monte Carlo simulation, using a Gaussian approximation for the distribution.⁹ The correction is non-negligible only for ${}^3\text{He}$ nuclei coincident with photons in the most forward backward detectors (corresponding to ${}^3\text{He}$ nuclei at the inner edge of the detector telescope), and the correction is $2\pm 1\%$ at the most forward angle and $1\pm 1\%$ at the most backward angle. The error in the solid angle was mostly due to an estimated uncertainty of 0.3 cm in the positioning of the lead collimators. Taking the average of the minimum and maximum corrections due to a non-normal orientation of the collimator face to the target ray gave an upward revision of $2.5\pm 2.5\%$ to account for this effect. An additional error of up to $\pm 2.3\%$ is possible if the collimator was shifted along the target detector axis. One more collimator correction is due to photon conversion in the inner edge of the collimator, causing the effective solid angle of the photon detector to be larger than its geometric value. These effects have been calculated, and we estimate that the real solid angle was 2% larger than the geometric solid angle at these energies.⁸ The carbon subtraction (which includes the random coincidence background) was 2.0 ± 0.5 nb/sr, giving a correction known to better than 0.25%. When all of these systematic uncertainties are added in quadrature, the total estimated error is $\pm 4.4\%$. The error budget is tabulated in Table I. An overall uncertainty in the normalization of 3% due to a possible error in measuring the target thickness (8.8 ± 0.3 mg/cm²) is not included.

TABLE I. Systematic error budget for the cross section.

Error source	Uncertainty (%)
TDC shifts	0.75
Multiple scattering	1.0
Photon detector efficiency	2.0
Photon conversion in collimator	1.0
rf sorting cut	0.5
Reaction effects in telescope	1.0
Carbon subtraction	0.25
Geometric effects: translation	2.3
Geometric effects: tilt	2.5
Errors added in quadrature	4.4

III. RESULTS

The results of this measurement are shown in Fig. 3. The error estimates of A_y and A_{yy} are statistical only, and do not include an overall 5% normalization uncertainty due to the polarimeter calibration. There are no other measurements of these analyzing powers at these energies. The error estimate for the cross section is the sum (in quadrature) of both the systematic (listed in Table I) and statistical uncertainties. At all angles the statistical error in the cross section is much smaller than the systematic error. The angular distribution of the cross section can be described as an expansion in Legendre polynomials of the form

$$\sigma(\theta) = A_0 \left[1 + \sum_{l=1} a_l P_l(\cos\theta) \right], \quad (1)$$

and the total cross section is then equal to $4\pi A_0$. Our value for the total cross section is $207 \pm 12 \mu\text{b}$ after conversion to the ${}^3\text{He}(\gamma, p){}^2\text{H}$ reaction using detailed balance. This value is slightly larger (15%) than that reported by Ticconi *et al.*,¹⁰ but the angular distribution of our measurement did not sufficiently constrain the fit at extreme angles. If arbitrary values of zero for $\sigma(0^\circ)$ and $\sigma(180^\circ)$ are added to the data set (with the typical error estimates of the other data points), then the total cross section is decreased by 10%, giving excellent agreement with the measurements of the inverse process.

In the following we compare the results of this measurement with the results of a simple two-body direct capture model.³ In this calculation the effects of the initial state interactions have been neglected, an assumption that should be more valid at this energy than at lower energies. The main approximation of this model is that in the electric multipole operators (EL) the deuteron is treated as a point particle. The position vector of the proton bound in the deuteron is then given by $\rho/3$ instead of $\rho/3 + \xi/2$ where $\rho = (\mathbf{r}_1 + \mathbf{r}_2)/2 - \mathbf{r}_3$ and $\xi = \mathbf{r}_1 - \mathbf{r}_2$ are the Jacobi coordinates of the three-body system. The dependence of the EL matrix elements on the internal structure of the ${}^3\text{He}$ ground state then arises exclusively from its projection into a deuteron and a proton since the EL operator becomes independent of ξ . This approximation does not affect the position vector of the spectator proton and its contribution to the EL operators. Only the $E1$ and $E2$ operators are included

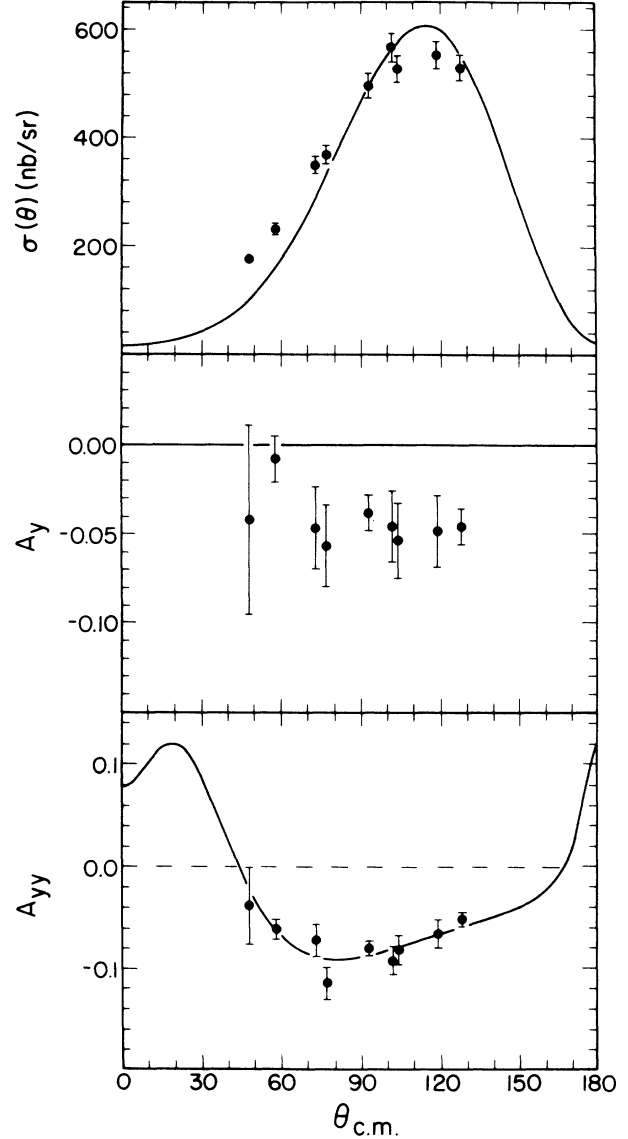


FIG. 3. Results for the ${}^1\text{H}(\vec{d}, \gamma){}^3\text{He}$ reaction at $E_d=95$ MeV ($E_\gamma=37$ MeV). The error estimates for $\sigma(\theta)$ include systematic error estimates while A_y and A_{yy} error estimates are statistical only. The solid curve is a PWBA model calculation, discussed in the text.

in this calculation, and explicit effects of meson exchange currents were not included. In this model

$$(EL)_{fi} \propto \sum_{j=1,2} \int (C_{j\rho})^L Y_{LM}(\hat{\rho}) \langle \psi_{3\text{He}} | \psi_d \chi_p \rangle e^{i\mathbf{p}\cdot\mathbf{r}} d\rho \quad (2)$$

where $C_1 = \frac{1}{3}$, $C_2 = -\frac{2}{3}$, and $e^{i\mathbf{p}\cdot\mathbf{r}}$ is considered to be the scattering p-d wave function for momentum \mathbf{p} . In particular, there are no contributions from the ${}^3\text{He}$ D -state component with orbital angular momentum $l_\rho = l_\xi = 1$. These components have a vanishing overlap with the positive parity deuteron ground state. The vertex function, $\langle {}^3\text{He} | \psi_d \chi_p \rangle$, is that of Sasakawa, taken from a Faddeev model calculation of ${}^3\text{H}$ using the Reid soft-core potential (Coulomb effects should not significantly

affect these results).¹¹ The wave functions were effectively antisymmetrized in the proton coordinate, since the antisymmetrization operator (which should be applied to the proton-deuteron state) can be applied to the ${}^3\text{He}$ wave function due to the symmetric nature of the electric operator. Since the ${}^3\text{He}$ wave function is already antisymmetric, the net effect of antisymmetrization is a constant. The asymptotic D - S state ratio η of the ${}^3\text{H}$ wave function of Sasakawa was determined by comparison to the asymptotic Hankel wave functions at 6 fm, and it was found that $\eta = -0.029$. This value of η is lower than that calculated from the unprojected Faddeev wave function. Later calculations gave $\eta = 0.039$ for the Paris potential and $\eta = -0.043$ when the effects of three-body forces are added.¹² In the asymptotic approximation, where the vertex function is replaced with the asymptotic Hankel functions, A_{yy} scales with η . At $E_\gamma = 3.8$ MeV, however, A_{yy} is sensitive to the interior of ${}^3\text{He}$, and thus η cannot be determined except as a parameter in a model calculation.

The results of the calculation are shown as a solid line in Fig. 3. The model describes the cross section at the maximum rather well, and D -state effects account for only a few percent of the cross section. Since distorted waves are not used in the calculation the predicted vector analyzing power A_y is identically zero, while the measured A_y has a small and negative non-zero value. Good agreement is found for the tensor analyzing power A_{yy} with the Sasakawa wave function. If the vertex function is a pure S state then A_{yy} vanishes; of the observed A_{yy} about 90% is from the ${}^3\text{He}$ D -state amplitude and the remaining 10% is due to the deuteron D -state amplitude.

IV. CONCLUSIONS

Previous measurements of the tensor analyzing power of radiative transitions in the three-body system have

been concentrated in an energy region where the initial state interaction is large. At the energy of this measurement this effect should be considerably less important, since the predicted cross section from the exact calculations and the DWBA give nearly identical results. We have interpreted our data using a plane-wave Born approximation (PWBA) model. This model gives an acceptable fit to our measurement of the tensor analyzing power, using a parameter set which also fits other measurements of A_{yy} at lower energies. The success of this approach in fitting the tensor analyzing powers, along with the results of Ref. 2, would seem to indicate that the assumptions of the direct capture description are largely valid. It is obviously necessary to confront these data with a complete calculation. Such a calculation has been carried out at $E_d = 29.2$ MeV, where it was found that the largest contribution to A_{yy} was from the $l_\rho = l_\xi = 1$ piece of the ${}^3\text{He}$ D state.¹ This is in sharp contradiction to the assumptions of the direct capture calculations. It is hoped that future theoretical work, extending the energy range for full three-body calculations, will resolve the question of which particular ${}^3\text{He}$ partition is responsible for generating the tensor analyzing power.

ACKNOWLEDGMENTS

The assistance and cooperation of P. T. Debevec, S. Lebrun, and A. M. Nathan of the University of Illinois is gratefully acknowledged. C. S. Yang and V. R. Cupps contributed to the early stages of this work. Support was furnished by the National Science Foundation as part of Grant 84-12177.

*Present address: University of Illinois, Urbana, IL 61801.

†Present address: Princeton University, Princeton, NJ 08544.

‡Present address: Los Alamos National Laboratory, Los Alamos, NM 87545.

§Present address: Fluehwiesenweg 5, CH-8116 Wuerenlos, Switzerland.

**Present address: University of North Carolina, Chapel Hill, NC 27514.

††Present address: University of Bonn, Bonn, Federal Republic of Germany.

‡‡Present address: University of the Western Cape, Belleville, South Africa.

¹J. Jourdan, M. Baumgartner, S. Burzynski, P. Egelhof, A. Klein, M. A. Pickar, G. R. Plattner, W. D. Ramsey, H. W. Roser, I. Sick, and J. Torre, Phys. Lett. **162B**, 269 (1986); J. Jourdan, M. Baumgartner, S. Burzynski, P. Egelhof, R. Henneck, A. Klein, M. A. Pickar, G. R. Plattner, W. D. Ramsey, H. W. Rose, I. Sick, and J. Torre, Nucl. Phys. **A453**,

220 (1986).

²M. C. Vetterli, J. A. Kuehner, A. J. Trudel, C. L. Woods, R. Dymarz, A. A. Pilt, and H. R. Weller, Phys. Rev. Lett. **54**, 1129 (1985).

³A. Arriaga and F. D. Santos, Phys. Rev. C **29**, 1945 (1984).

⁴B. F. Gibson and D. R. Lehman, Phys. Rev. C **11**, 29 (1975).

⁵I. M. Barbour and A. C. Phillips, Phys. Rev. C **1**, 165 (1970).

⁶Indiana University Cyclotron Facility Annual Report No. 7, 1982 (unpublished), p. 163.

⁷R. M. DeVries and J. C. Peng, Phys. Rev. C **22**, 1055 (1980).

⁸M. A. Pickar, Ph.D. thesis, Indiana University, 1982.

⁹V. L. Highland, Nucl. Instrum. Methods **129**, 497 (1975); **161**, 171 (1979).

¹⁰G. Ticconi, S. N. Gardiner, J. L. Matthews, and R. O. Owens, Phys. Lett. **46B**, 369 (1973).

¹¹T. Sasakawa and T. Sawada, Phys. Rev. C **19**, 2035 (1979).

¹²S. Ishikawa and T. Sasakawa, Phys. Rev. Lett. **56**, 317 (1986).